

Synthesis of four-, five-, and six-coordinate cobalt(III) bis-*o*-iminobenzosemiquinone complexes*

A. V. Piskunov,^{a*} K. I. Pashanova,^a I. V. Ershova,^a A. S. Bogomyakov,^b A. G. Starikov,^c and A. V. Cherkasov^d

^aG. A. Razuvaev Institute of Organometallic Chemistry, Russian Academy of Sciences, 49 ul. Tropinina, 603950 Nizhny Novgorod, Russian Federation.
Fax: +7 (831) 462 7497. E-mail: pial@iomc.ras.ru

^bInternational Tomography Center, Siberian Branch of the Russian Academy of Sciences, 3a ul. Institutskaya, 630090 Novosibirsk, Russian Federation

^cInstitute of Physical and Organic Chemistry, Southern Federal University, 194/2 prosp. Stachki, 344090 Rostov-on-Don, Russian Federation

Cobalt(III) complexes with different 4,6-di-*tert*-butyl-*N*-(aryl)-*o*-iminobenzosemiquinone ligands were synthesized. Four-, five-, or six-coordinate cobalt(III) derivatives can be prepared using various starting metal compounds (CoCl₂·6H₂O, (acac)₂Co·2H₂O) and varying substituents in the *N*-aryl moiety of the organic ligand. The structures of five synthesized compounds were determined by X-ray diffraction. The electronic and spin states of the five-coordinate cobalt(III) complexes were studied in detail by DFT quantum chemical calculations.

Key words: *o*-iminobenzosemiquinone, cobalt(III), X-ray diffraction, DFT method.

Coordination and organometallic compounds containing redox-active ligands have attracted increasing attention of researchers and represent a promising growth area of modern chemistry.¹ This class of compounds has found considerable interest due mainly to their unique chemical and magnetic properties imparted by the introduction of organic ligands capable of changing the oxidation state in the coordination sphere of the metal center. A series of recent studies showed that metal complexes with such ligand systems hold promise in stoichiometric and catalytic transformations of organic and inorganic substrates.^{2–10} *o*-Aminophenols (*o*-iminobenzoquinones) and their numerous functionalized derivatives belong to the most popular redox-active ligand systems.¹¹ Among a plenty of transition¹¹ and main-group^{12–15} metal compounds based on this type of ligands, noteworthy are cobalt complexes capable of catalyzing the Negishi cross-coupling reaction.¹⁶ The first cobalt(III) compound containing three *o*-iminobenzosemiquinone radical-anion ligands was synthesized in 1999 by the reaction of cobalt(II) chloride with 4,6-di-*tert*-butyl-*N*-phenyl-*o*-aminophenol in the presence of atmospheric oxygen.¹⁷ In subsequent years, this procedure was successfully applied to the synthesis of a number of four-coordinate cobalt derivatives containing two *o*-iminobenzoquinone-type ligands.^{18–20} However, cobalt(II) perchlorate is most commonly utilized as a source

of cobalt ions in reactions with substituted *o*-aminophenols used to synthesize homoleptic *o*-iminobenzoquinone complexes.^{21–24} It should be noted that the reactions of different cobalt(II) salts with *o*-aminophenols functionalized by additional donor groups in the *N*-aryl moiety can involve side processes, resulting in transformations of redox-active ligands.^{25–28} Besides, recent studies demonstrated that the reactions of some *o*-aminophenols with cobalt(II) chloride can be accompanied by the formation of five-coordinate compounds of this metal containing a halide ion²⁴ (pseudohalide ion²⁹) along with two *o*-iminobenzoquinone-type ligands. The latter metal complexes are of particular interest because they exhibit catalytic properties in transformations of aryl isocyanates into diaryl urea.²⁴ Therefore, *o*-iminobenzoquinone ligand systems can impart additional redox and acid-base properties to the cobalt compounds, which is of great importance for the formation of new catalytic systems.³⁰

In the present study, we tested new synthetic approaches to the preparation of cobalt(III) complexes based on three *o*-aminophenols containing substituents of different nature in the *N*-aryl moiety. Four-, five-, and six-coordinate cobalt(III) bis-*o*-iminobenzosemiquinonates were synthesized and characterized.

Results and Discussion

Synthesis of *o*-iminobenzoquinone complexes. According to the literature data,^{17–29} the reaction of different cobalt

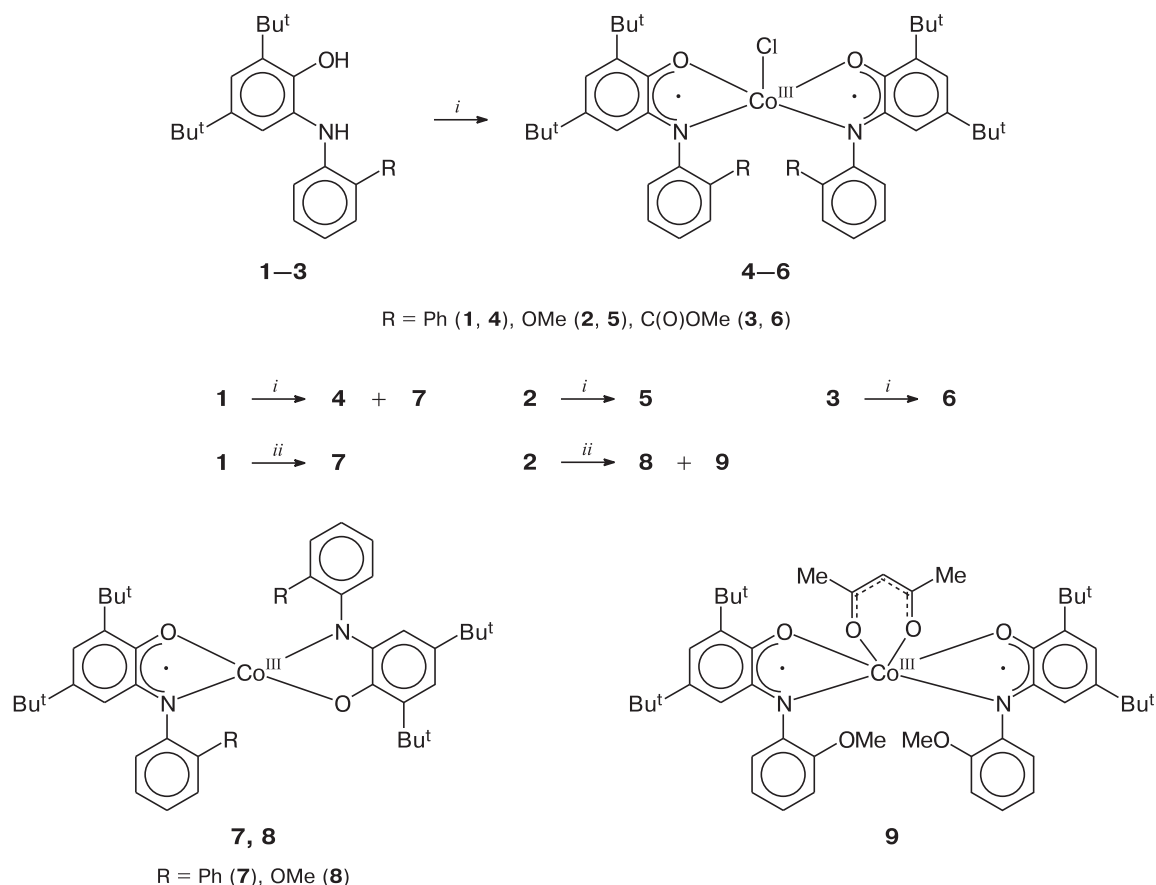
* Based on the materials of the Russian National Cluster of Conferences on Inorganic Chemistry "InorgChem-2018" (September 17–21, 2018, Astrakhan, Russia).

salts with *o*-aminophenols in the presence of atmospheric oxygen and bases is the most commonly used synthetic approach to the preparation of *o*-iminobenzoquinone derivatives of this metal. Besides, it was recently shown²⁰ that this reaction with cobalt(II) chloride performed in two steps, including the reaction of the metal salt with an organic ligand in the presence of triethylamine under inert conditions followed by the treatment of the reaction mixture with atmospheric oxygen, ensures higher yields of the analytically pure target product. We tested this modified procedure using the reactions of cobalt(II) chloride with 4,6-di-*tert*-butyl-*N*-(diphenyl)-*o*-aminophenol (**1**), 4,6-di-*tert*-butyl-*N*-(2-methoxyphenyl)-*o*-aminophenol (**2**), and methyl 2-(3,5-di-*tert*-butyl-2-hydroxyphenylamino)benzoate (**3**) (Scheme 1). The reaction in methanol (as applied to derivative **4**) or acetonitrile (in the case of compounds **5** and **6**) followed by the treatment of the reaction mixture with atmospheric oxygen is completed overnight at room temperature and is accompanied by the formation of intensely colored blue solutions, from which five-coordinate complexes **4–6** of the composition

(ISQ)₂Co^{III}Cl (ISQ is the radical-anion of the corresponding *o*-iminobenzoquinone) gradually crystallize.

The molecular formula analysis of the crystalline phase isolated in the reaction showed that compounds **5** and **6** are analytically pure, whereas derivative **4**, prepared by the reaction of cobalt chloride with compound **1**, contains an impurity of four-coordinate complex **7**. The presence of compound **7** in the reaction products was established by recording anisotropic ESR spectra²⁴ in the frozen dichloromethane matrix. Since components of the reaction mixture have a similar solubility in most organic solvents, we failed to isolate the products of this reaction in the individual state. This fact is in good agreement with the results of the previous studies,²⁴ and this procedure is inapplicable to the targeted synthesis of complexes **4** and **7**. Crystals of compounds **4–6** suitable for X-ray diffraction were obtained by slow crystallization directly from the reaction mixtures. It should be noted that compound **4** was previously characterized by single-crystal X-ray diffraction at *T* = 293 K.²⁴ We collected the X-ray diffraction data set from single crystals of complex **4** at *T* = 100 K.

Scheme 1



i. 1) CoCl₂ · 6 H₂O, Et₃N; 2) O₂; *ii.* 1) (acac)₂Co · 2 H₂O; 2) O₂,

Measurements of the temperature dependences of magnetic susceptibility showed that complexes **5** and **6** possess only residual paramagnetism at 300 K. The magnetic moment decreases to zero with decreasing temperature. For compound **5**, we succeeded in recording the well-resolved solution NMR spectrum even at room temperature.

In order to exclude processes giving a mixture of five- and four-coordinate cobalt *o*-iminobenzoquinone complexes, we tested a new approach in the chemistry of this class of compounds, including the employment of metal acetylacetonate instead of its chloride. In this case, the addition of NEt_3 to the reaction mixture is not required for binding HCl . The reaction mixture of compound **1** and $(\text{acac})_2\text{Co} \cdot 2\text{H}_2\text{O}$ was heated for a few hours on a water bath, and then atmospheric oxygen was introduced into the tube, resulting in intense blue coloration. Analytically pure dark-blue crystalline complex **7** (see Scheme 1) was isolated after overnight. The composition of **7** was confirmed by IR, ESR, and UV-Vis spectroscopy compared to the parameters determined in the previous study²⁴ and by elemental analysis. The molecular and crystal structure of complex **7** was determined by X-ray diffraction.

The above-described synthetic approach is not universal. Thus, the crystalline phase isolated from the reaction mixture after the similar reaction involving compound **2** is not an individual substance. The results of elemental analysis of the reaction product are in satisfactory agreement with the calculated contents of elements for compound **8**, whereas the X-ray diffraction study of the single crystals obtained by slow crystallization from the reaction mixture revealed the presence of six-coordinate complex **9** (see Scheme 1).

Molecular structure of 7. The cobalt atom in complex **7** exhibits a distorted square-planar coordination geometry ($\tau_4 = 0.05$).³¹ Like in the copper(II) derivative,³² the phenyl moieties of biphenyl substituents of the ligands are *cis*-ori-

ented with respect to the $\text{N}(1)\text{O}(1)\text{N}(2)\text{O}(2)$ plane (Fig. 1). The dihedral angle between the planes of the ligands in complex **7** ($7.1(2)^\circ$) is somewhat smaller than that in the copper(II) complex. In the crystal packing of complex **7**, there is a weak π – π interaction between the biphenyl moieties (Fig. 2). The shortest distance between the biphenyl carbon atoms of adjacent molecules is $3.51(2)$ Å.

The conjugation with the equidistant C–C bonds is retained for the phenyl rings of the aniline moiety of the ligands, while the quinoid distortion is observed for the phenyl rings containing *tert*-butyl substituents (two short and four long C–C distances), which is typical of the radical-anion form of *o*-iminobenzoquinone-type ligands (Table 1). The corresponding C–C bond lengths in these phenyl groups are relatively averaged. However, noteworthy is a considerable elongation of the $\text{C}(5)$ – $\text{C}(6)$ ($1.395(2)$ Å) and $\text{C}(31)$ – $\text{C}(32)$ ($1.391(2)$ Å) bonds. Besides, the short bond lengths ($1.387(2)$ and $1.389(2)$ Å) are somewhat larger compared to the typical distribution (~ 1.360 – 1.385 Å) for the corresponding bonds in *o*-iminobenzosemiquinones.³³ The C–O ($1.326(2)$ – $1.331(2)$ Å) and C–N ($1.370(2)$ – $1.376(2)$ Å) distances have intermediate values between those characteristic of the radical-anion (C–O, 1.30 Å; C–N, 1.35 Å)³³ and deprotonated *o*-amidophenolate (C–O, 1.35 Å; C–N, 1.38 Å)³³ forms of *o*-iminobenzoquinone ligand systems. The calculated metrical oxidation states (MOS)³³ are -1.49 ± 0.03 and -1.45 ± 0.05 , which are also intermediate between those expected for *o*-iminobenzosemiquinone and *o*-amidophenolate (with a closed shell) forms (-1 and -2 , respectively). The above facts hinder a definite determination of the oxidation state of the ligands. Hence, the question arises as to the oxidation state of the metal center.

Examples of planar four-coordinate cobalt derivatives containing the metal ion in the oxidation state +3 and differently charged ligands (one ligand in the radical-

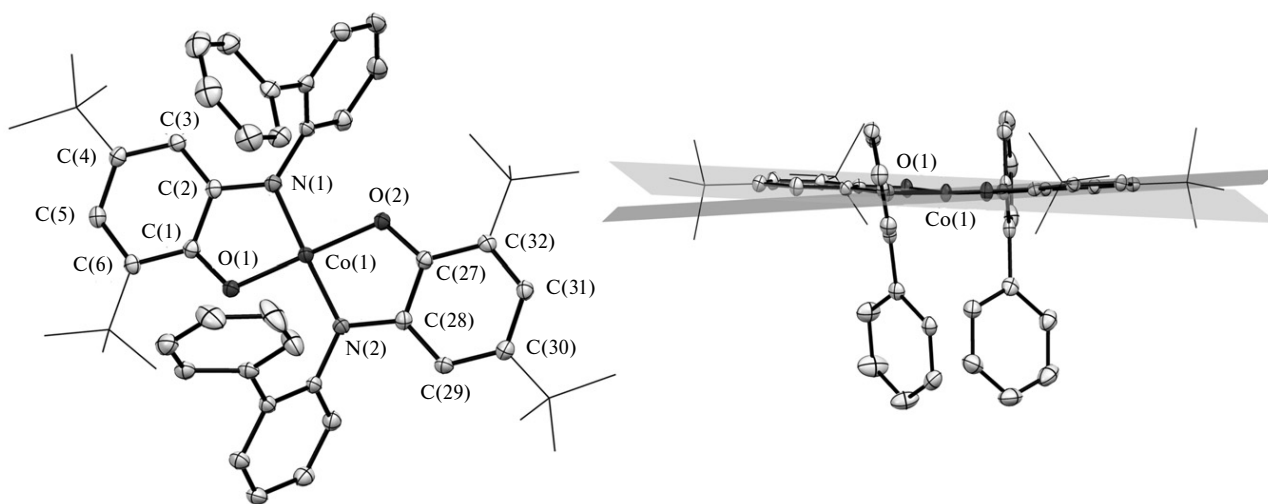


Fig. 1. Molecular structure of complex **7** with displacement ellipsoids drawn at the 50% probability level. Hydrogen atoms are not shown.

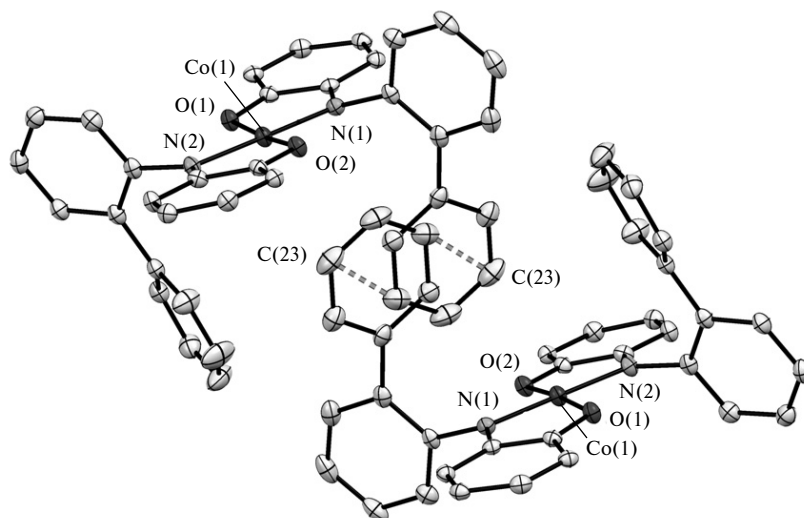


Fig. 2. Fragment of the crystal structure of complex **7** with displacement ellipsoids drawn at the 50% probability level. Hydrogen atoms and *tert*-butyl groups are not shown.

anion form and another ligand in the deprotonated *o*-amidophenolate oxidation state) were described in the literature.^{19,21,24} The C—O distances and short C—C bond lengths in these metal complexes are also larger than the expected values³³ for *o*-iminobenzosemiquinone ligands and are in good agreement with those found in complex **7**. The trivalent state of the metal center is evidenced by the cobalt—heteroatom bond lengths (Co—O, 1.819(2),

1.826(2) Å; Co—N, 1.832(2), 1.845(2) Å), which are comparable with the Co—O and Co—N distances in the planar Co^{III} complexes described previously.^{19,21,24}

The ESR spectroscopic data²⁴ for metal complex **7** indicate that the unpaired electron is localized on the metal center and are in good agreement with the results of relevant studies performed in the present work at $T = 150$ K. The doublet ground spin state ($S = 1/2$) of compound **7**

Table 1. Selected bond lengths (d) for complexes **4** and **7**

Bond	$d/\text{Å}$	Bond	$d/\text{Å}$	Bond	$d/\text{Å}$
Complex 4		Complex 4 *		Complex 7	
Co(1)—Cl(1)	2.2687(7)	Co(1)—Cl(1)	2.2661(9)	Co(1)—O(1)	1.826(2)
Co(1)—O(1)	1.853(2)	Co(1)—O(1)	1.855(2)	Co(1)—N(1)	1.832(2)
Co(1)—N(1)	1.875(2)	Co(1)—N(1)	1.873(2)	Co(1)—O(2)	1.819(2)
Co(1)—O(2)	1.870(2)	Co(1)—O(2)	1.869(2)	Co(1)—N(2)	1.845(2)
Co(1)—N(2)	1.861(2)	Co(1)—N(2)	1.865(2)	O(1)—C(2)	1.331(2)
O(1)—C(1)	1.296(3)	O(1)—C(2)	1.300(3)	N(1)—C(1)	1.370(2)
N(1)—C(2)	1.346(3)	N(1)—C(1)	1.341(3)	O(2)—C(27)	1.326(2)
O(2)—C(27)	1.297(3)	O(2)—C(28)	1.291(3)	N(2)—C(28)	1.376(2)
N(2)—C(28)	1.340(3)	N(2)—C(27)	1.337(3)	C(1)—C(2)	1.423(2)
C(1)—C(2)	1.435(3)	C(1)—C(2)	1.434(4)	C(1)—C(3)	1.409(2)
C(2)—C(3)	1.413(3)	C(1)—C(6)	1.417(4)	C(3)—C(4)	1.389(2)
C(3)—C(4)	1.373(3)	C(5)—C(6)	1.368(4)	C(4)—C(5)	1.412(2)
C(4)—C(5)	1.434(3)	C(4)—C(5)	1.430(4)	C(5)—C(6)	1.395(2)
C(5)—C(6)	1.372(3)	C(3)—C(4)	1.370(4)	C(2)—C(6)	1.411(2)
C(1)—C(6)	1.431(3)	C(2)—C(3)	1.425(4)	C(27)—C(28)	1.417(2)
C(27)—C(28)	1.435(3)	C(27)—C(28)	1.443(4)	C(28)—C(29)	1.409(2)
C(28)—C(29)	1.420(3)	C(27)—C(32)	1.416(4)	C(29)—C(30)	1.387(2)
C(29)—C(30)	1.363(3)	C(31)—C(32)	1.358(4)	C(30)—C(31)	1.414(2)
C(30)—C(31)	1.433(3)	C(30)—C(31)	1.446(4)	C(31)—C(32)	1.391(2)
C(31)—C(32)	1.371(3)	C(29)—C(30)	1.368(4)	C(27)—C(32)	1.414(2)
C(27)—C(32)	1.440(3)	C(28)—C(29)	1.433(4)		

* Literature data²⁴ (X-ray diffraction study was performed at $T = 293$ K).

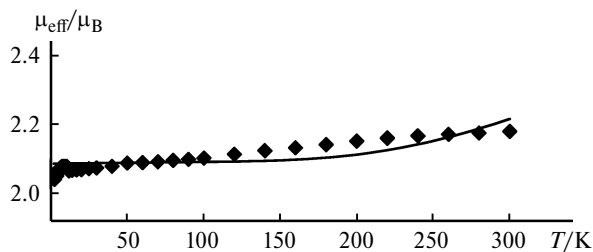


Fig. 3. Experimental (dots) and theoretical (curve) temperature dependences $\mu_{\text{eff}}(T)$ for a polycrystalline sample of complex **7** ($J < -300 \text{ cm}^{-1}$).

is confirmed by the results of magnetochemical studies (Fig. 3). The effective magnetic moment (μ_{eff}) at 300 K is $2.18 \mu_{\text{B}}$, and it slightly changes with decreasing temperature. The μ_{eff} value in the temperature range of 2–300 K is higher than the theoretical spin-only value ($1.73 \mu_{\text{B}}$) expected for a system containing one unpaired electron with the g -factor equal to 2 and is well consistent with the value of $2.141 \mu_{\text{B}}$ taking into account that the g -tensor values (1.980; 2.020; 3.215)²⁴ are larger than the spin-only value ($g_{\text{av}} = 2.405$). The observed character of the dependence $\mu_{\text{eff}}(T)$ attests to the presence of strong antiferromagnetic exchange interactions between the spins of the Co^{3+} ion ($S_{\text{Co}} = 1$) and the *o*-iminobenzosemiquinone radical ($S_{\text{R}} = 1/2$) and the absence of significant intermolecular exchange interactions. An analysis of the experimental dependence $\mu_{\text{eff}}(T)$ for complex **7** in terms of the exchange-coupled dimer model (Hamiltonian $H = -2J \cdot S_{\text{Co}} \cdot S_{\text{R}}$) provides an estimate of the metal–ligand magnetic exchange energy at $J < -300 \text{ cm}^{-1}$.

Therefore, based on the analysis of the structural parameters of compound **7** and the results of magnetochemical studies and ESR spectroscopy,²⁴ it can be concluded that compound **7** contains a cobalt(III) ion and two

o-iminobenzoquinone ligands in different redox states (radical-anion and dianion). The charge transfer between differently charged redox-active ligands appears as a broad absorption band in the near-IR region at 1150–2100 nm with a maximum at $\lambda = \sim 1686 \text{ nm}$.

Molecular structures of complexes 4–6. The coordination environment of the cobalt atom in five-coordinate complexes **4–6** is a distorted ($\tau_5(\mathbf{4}) = 0.02$, $\tau_5(\mathbf{5}) = 0.13$, and $\tau_5(\mathbf{6}) = 0.04$)³⁴ tetragonal pyramid (Figs 4 and 5). The base of the pyramid is formed by O and N atoms of *o*-iminobenzosemiquinone ligands, and the apical position is occupied by the Cl atom. The dihedral angles between the planes of *o*-iminobenzosemiquinone ligands in structures **4–6** are in the range of 9.1(2)–13.8(2)°. The deviation of the Co atom from the plane formed by the N and O atoms of the metallocycles is smaller than 0.29(2) Å (Table 2). The functional groups (Ph, OMe, C(O)OMe) in the *ortho* positions of *N*-aryl moieties of the ligands are on the same side of the base of the pyramid.

As in the four-coordinate Co^{III} derivative (**7**), there are weak π – π interactions between the biphenyl moieties (C...C, 3.57(2)–3.66(2) Å) in complex **4**. A comparative analysis of the geometric characteristics of compound **5** and the four-coordinate Cu^{II} and Ni^{II} complexes containing a similar ligand system³⁵ suggests a continuing tendency toward the existence of weak coordination to the metal center of only one of the two OMe groups. This is supported by the fact that the Co(1)–O(2) distance (3.50(2) Å) is consistent with the sum of the van der Waals radii of the corresponding elements (3.5 Å),³⁶ whereas the Co(1)–O(4) distance (4.09(2) Å) is substantially larger than this value. In metal complex **6**, weak interactions between the Co^{3+} ion and carbomethoxy groups are absent, the spatial arrangement of these groups being different. Thus, one C(O)OMe group forms a shorter contact with the metal center *via* the methoxy oxygen atom

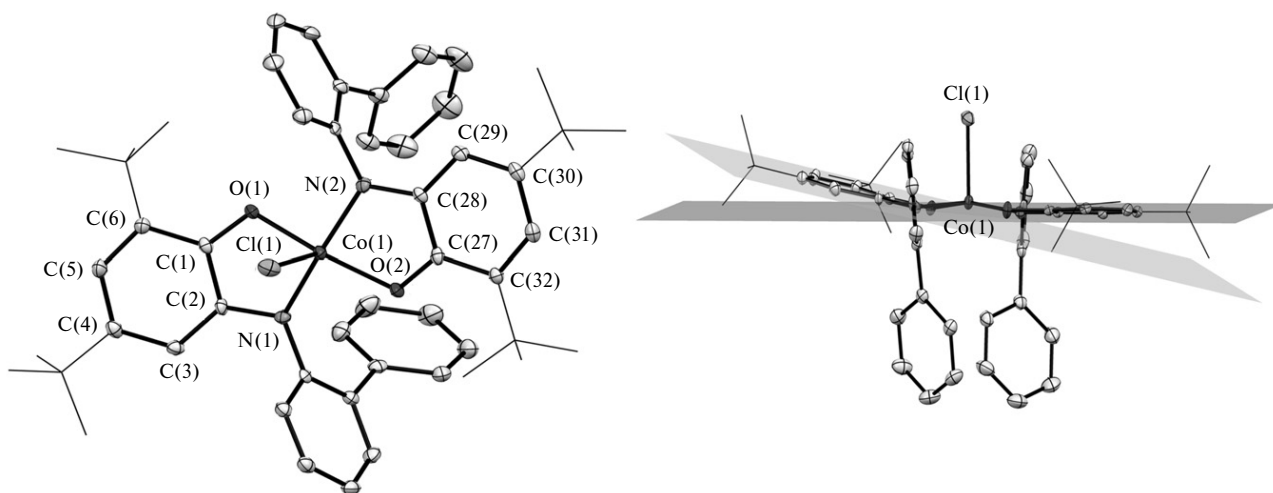


Fig. 4. Molecular structure of complex **4** with displacement ellipsoids drawn at the 50% probability level. Hydrogen atoms are not shown.

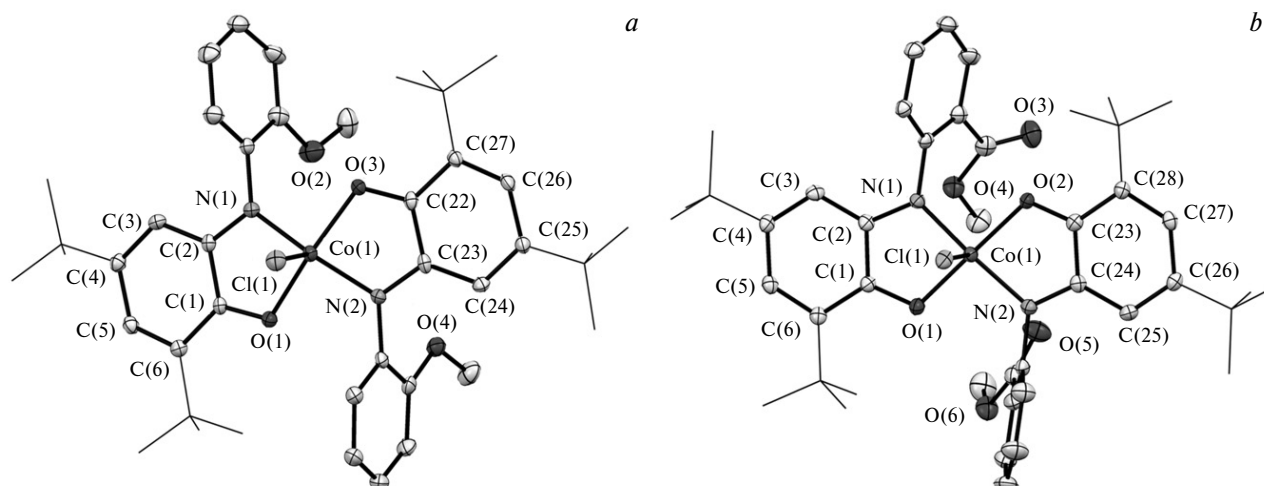


Fig. 5. Molecular structures of complexes **5** (a) and **6** (b) with displacement ellipsoids drawn at the 50% probability level. Hydrogen atoms are not shown.

(Co(1)...O(4), 3.52(2) Å), whereas the carbonyl oxygen atom of another group is involved in the shorter contact with the metal (Co(1)...O(5), 3.60(2) Å). For comparison, the four-coordinate Cu^{II} and Ni^{II} derivatives are characterized by the coordination of both potentially chemilabile C(O)OMe groups to the metal ion through the oxygen atoms of C=O groups.³⁵

The geometric characteristics of complexes **4–6** determined by X-ray diffraction are summarized in Tables 1–4. In all these five-coordinate compounds, organic ligands are in the radical-anion redox form, and the metal center is in the trivalent state (Co^{III}, d⁶). This is confirmed by the fact that the calculated oxidation states of the ligands in compounds **4–6** are very similar and have the following values: MOS(**4**) = -0.96 ± 0.05 and -0.92 ± 0.07 ; MOS(**5**) = -0.95 ± 0.06 and -0.83 ± 0.07 ; MOS(**6**) = -0.90 ± 0.04 and -0.90 ± 0.05 . The quinoid distortion of the *tert*-butyl-substituted phenyl rings typical of *o*-imino-

benzosemiquinones is characterized by the following lengths of short C–C bonds: 1.363(3)–1.373(3) Å for **4**, 1.359(6)–1.373(6) Å for **5**, and 1.364(4)–1.375(4) Å for **6**. In turn, the long C–C distances are in the ranges of 1.420(3)–1.440(3) Å (**4**), 1.422(6)–1.437(6) Å (**5**), and 1.419(4)–1.439(4) Å (**6**). Another well-known distinguishing feature of the radical-anion oxidation state of the *o*-iminobenzoquinone-type ligand systems is carbon–heteroatom distances (C–O and C–N) of chelate rings intermediate between those for single and double bonds. This feature is observed also in compounds **4–6** (for **4**, C–O, 1.296(3), 1.297(3) Å; C–N, 1.340(3), 1.346(3) Å; for **5**, C–O, 1.287(5), 1.296(5) Å; C–N, 1.342(5), 1.346(5) Å; for **6**, C–O, 1.291(3), 1.296(3) Å; C–N, 1.342(3), 1.346(4) Å). As mentioned above, the central cobalt ion in compounds **4–6** is in the trivalent state, which is evidenced by the metal–heteroatom bond lengths (for **4**, Co–O, 1.853(2), 1.870(2) Å; Co–N, 1.861(2), 1.875(2) Å; for **5**, Co–O, 1.874(3), 1.878(3) Å; Co–N, 1.858(3), 1.859(4) Å; for **6**, Co–O, 1.860(2), 1.862(2) Å; Co–N, 1.862(2), 1.869(2) Å). These distances are comparable with the corresponding bond lengths in related five-coordinate Co^{III} complexes having a tetragonal-pyramidal coordination and containing different anionic ligands as substituents.^{16,19,24,37–39}

Table 2. Selected bond angles (ω) for complexes **4** and **7**

Angle	ω/deg		
	4	4*	7
O(1)–Co(1)–N(2)	93.53(7)	93.64(9)	95.43(5)
O(1)–Co(1)–O(2)	168.67(7)	168.71(9)	175.28(5)
N(2)–Co(1)–O(2)	84.00(7)	83.70(9)	85.87(5)
O(1)–Co(1)–N(1)	83.97(7)	83.94(9)	86.18(5)
N(2)–Co(1)–N(1)	167.48(8)	167.3(2)	178.14(5)
O(2)–Co(1)–N(1)	96.05(7)	96.25(9)	92.46(5)
O(1)–Co(1)–Cl(1)	92.22(5)	93.43(7)	—
N(2)–Co(1)–Cl(1)	97.41(6)	97.23(7)	—
O(2)–Co(1)–Cl(1)	99.06(5)	97.78(7)	—
N(1)–Co(1)–Cl(1)	94.94(6)	95.32(7)	—

* Literature data²⁴ (X-ray diffraction study was performed at $T = 293$ K).

Molecular structure of complex 9. Complex **9** crystallizes in space group $C2/c$. There is one molecule of the complex per asymmetric unit (Fig. 6), which occupies a special position on a twofold axis. The coordination environment of the Co³⁺ cation is a distorted octahedron. The equatorial plane is formed by O atoms of the acetylacetonate ligand and N atoms, and the apical positions are occupied by O atoms of the *o*-iminobenzo-semiquinone ligands. The N–Co–O and N–Co–N bond angles are close to 90°. The geometric characteristics of the redox-active ligands are given in Tables 3 and 4 and unambigu-

Table 3. Selected bond lengths (*d*) for complexes **5**, **6**, and **9**

Bond	<i>d</i> /Å	Bond	<i>d</i> /Å	Bond	<i>d</i> /Å	
Complex 6						
Co(1)—Cl(1)	2.2960(8)	C(25)—C(26)	1.364(4)	C(5)—C(6)	1.370(6)	
Co(1)—O(2)	1.860(2)	C(26)—C(27)	1.435(4)	C(1)—C(6)	1.434(6)	
Co(1)—O(1)	1.862(2)	C(27)—C(28)	1.372(4)	C(22)—C(23)	1.436(6)	
Co(1)—N(2)	1.869(2)	C(23)—C(28)	1.435(4)	C(23)—C(24)	1.422(6)	
Co(1)—N(1)	1.862(2)	Complex 5				
O(1)—C(1)	1.296(3)	Co(1)—Cl(1)	2.262(2)	C(25)—C(26)	1.437(6)	
N(1)—C(2)	1.342(3)	Co(1)—O(3)	1.878(3)	C(26)—C(27)	1.365(6)	
O(2)—C(23)	1.291(3)	Co(1)—O(1)	1.874(3)	C(22)—C(27)	1.441(6)	
N(2)—C(24)	1.346(4)	Co(1)—N(2)	1.859(4)	Complex 9		
C(1)—C(2)	1.439(4)	Co(1)—N(1)	1.858(3)	Co(1)—O(1)	1.874(2)	
C(2)—C(3)	1.417(4)	O(1)—C(1)	1.296(5)	Co(1)—N(1)	1.928(2)	
C(3)—C(4)	1.364(4)	N(1)—C(2)	1.346(5)	O(1)—C(2)	1.310(2)	
C(4)—C(5)	1.435(4)	O(3)—C(22)	1.287(5)	N(1)—C(1)	1.390(2)	
C(5)—C(6)	1.375(4)	N(2)—C(23)	1.342(5)	C(1)—C(2)	1.408(3)	
C(1)—C(6)	1.429(4)	C(1)—C(2)	1.432(6)	C(1)—C(6)	1.401(2)	
C(23)—C(24)	1.439(4)	C(2)—C(3)	1.432(6)	C(5)—C(6)	1.380(3)	
C(24)—C(25)	1.419(4)	C(3)—C(4)	1.373(6)	C(4)—C(5)	1.399(3)	
		C(4)—C(5)	1.431(6)	C(3)—C(4)	1.375(3)	
				C(2)—C(3)	1.414(2)	

Table 4. Selected bond angles (ω) for complexes **5**, **6**, and **9**

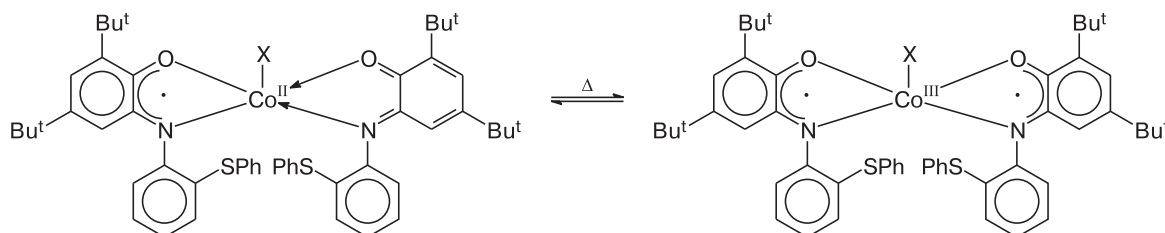
Angle	ω /deg		Angle	ω /deg	Angle	ω /deg
	6	5				
N(2)—Co(1)—N(1)	166.1(2)	158.4(2)	Complex 6			
N(2)—Co(1)—O(1)	95.62(9)	92.9(2)	N(2)—Co(1)—O(2)	83.86(9)	Complex 5	
N(1)—Co(1)—O(1)	83.59(9)	83.7(2)	N(1)—Co(1)—O(2)	94.13(9)	O(1)—Co(1)—O(3)	166.1(2)
N(2)—Co(1)—Cl(1)	97.61(7)	101.0(2)	O(1)—Co(1)—O(2)	168.40(8)	O(3)—Co(1)—Cl(1)	98.0(2)
N(1)—Co(1)—Cl(1)	96.27(7)	100.6(2)	O(2)—Co(1)—Cl(1)	97.83(6)	Complex 9	
O(1)—Co(1)—Cl(1)	93.72(6)	95.9(2)	Complex 5			
			N(1)—Co(1)—O(1)	83.7(2)	N(1A)—Co(1)—N(1)	90.7(2)
			N(1)—Co(1)—O(3)	94.5(2)	N(1A)—Co(1)—O(1)	94.18(6)
					N(1)—Co(1)—O(1)	85.18(6)
					O(1)—Co(1)—O(1A)	179.08(8)

ously characterize their oxidation state as the radical-anion one (the detailed analysis was performed for complexes **4–7**). The bond lengths and bond angles in the acetylacetonate ligand are similar to those in cobalt(III) acetylacetonates.⁴⁰

Study of the electronic and spin states of complex 5 by the DFT method. It was suggested²⁹ that five-coordinate cobalt complexes can exhibit redox isomerism (Scheme 2).

Hence, a decrease in the temperature would be expected to cause the formation of a cobalt(II) compound containing redox-active ligands in the neutral and radical-anion states.

This is a fairly unexpected statement because both the spectroscopic and X-ray diffraction data for compounds with the general formula (ISQ)₂CoX obtained previously^{16,19,24,37–39} provided no basis for this conclusion. To determine the electronic structure of this type of com-

Scheme 2

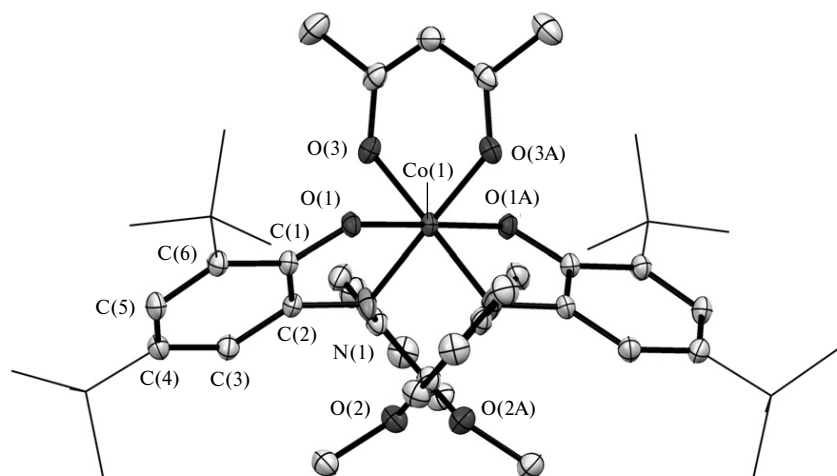


Fig. 6. Molecular structure of complex **9** with displacement ellipsoids drawn at the 50% probability level. Hydrogen atoms are not shown.

pounds, we studied isomers of compound **5** by the DFT method at the UB3LYP*/6-311++G(d,p) level of theory. All calculations were carried out using model structures, in which the *tert*-butyl groups were replaced by hydrogen atoms. The geometry optimization of the complex on the singlet PES using the unrestricted DFT method resulted in the location of two structures. In one of them, the spin density on the cobalt ion is absent, while the *o*-imino-benzoquinone ligands each have a single unpaired electron with an antiparallel spin alignment (Fig. 7, structure **5a**). Consequently, structure **5a** represents the broken-symmetry (BS) state of the electromer⁴¹ ISQ-_{LS}Co^{III}-ISQ. The value of the operator S^2 , which is underestimated compared to the expected value (Table 5), is due to strong antiferromagnetic exchange interactions.⁴² One unpaired electron is present on each organic ligand of the second electromer (**5b**). These electrons are antiferromagnetically coupled to unpaired electrons of the trivalent cobalt ion in an intermediate spin state (ISQ-_{IS}Co^{III}-ISQ). Structure **5c** having three unpaired electrons on the metal ion corresponds to

Table 5. Total energy (E_{total}), spin-squared operator S^2 , exchange interaction parameter (J), and relative energy (ΔE) of isomers of model complex **5** calculated by the DFT method at the UB3LYP*/6-311++G(d,p) level of theory

Structure*	$-E_{\text{total}}$ /au	S^2	$J_{\text{ISQ-ISQ/Co-ISQ}}$ /cm ⁻¹	ΔE /kcal mol ⁻¹
$\alpha\alpha$ - 5a	3256.65233	2.261	—	—
$\beta\alpha$ - 5a	3256.66784	0.520	-1955	0.4
$\alpha\alpha\alpha$ - 5b	3256.64372	6.035	—	—
$\beta\alpha\alpha$ - 5b	3256.66136	2.615	-1453/-1036	—
$\alpha\beta\alpha$ - 5b	3256.66853	0.777	—	0.0
$\alpha\alpha$ - 5c	3256.65614	6.174	—	—
$\beta\alpha$ - 5c	3256.66578	3.043	-676	1.7

* α is spin up, β is spin down.

another thermally accessible isomer. Taking into account the delocalization of one unpaired electron over the ligand system (see Fig. 7), the ISQ-_{HS}Co^{II}-IQ state can be assigned to this structure. This state includes the high-spin divalent metal ion and redox-active ligands in the neutral and radical-anion oxidation states.

An insignificant energy difference between structures **5b** and **5c** (1.7 kcal mol⁻¹) attests to the possible valence tautomerism in complex **5**; however, the transition of the isomer ISQ-_{HS}Co^{II}-IQ to the BS state involving two unpaired electrons would not be expected taking into account the diamagnetism of this compound.

Experimental

o-Aminophenols **1**,³² **2**,⁴³ and **3** (see Ref. 35) were synthesized by known procedures. The commercial reagents CoCl₂·6H₂O (Aldrich), (acac)₂Co·2H₂O (Aldrich), triethylamine (Aldrich), and I₂ (special purity grade 20-3, TU 6-09-2545-77) were used as received. The solvents used in experiments were purified and dehydrated according to standard procedures.⁴⁴

The IR spectra were recorded on a FSM-1201 Fourier-transform infrared spectrometer (4000–450 cm⁻¹ region) as Nujol mulls in KBr cells. Elemental analysis (C, H) was carried out on a Euro EA 3000 elemental analyzer. The ESR spectra were recorded on a Bruker EMX spectrometer operating at ~9.7 GHz. The *g*-factors were determined using diphenylpicrylhydrazyl (*g* = 2.0037) as the standard. The NMR spectra were measured on a Bruker DPX-200 spectrometer (200 MHz) with tetramethylsilane as the internal standard. Magnetic susceptibility measurements for a polycrystalline sample of **7** were performed on a Quantum Design MPMSXL SQUID magnetometer (magnetic field 0.5 T) in the temperature range of 2–300 K.

Computational methods. Calculations were carried out using the Gaussian 09 package⁴⁵ by the density functional theory (DFT) method at the B3LYP*/6-311++G(d,p) level of theory,⁴⁶ which correctly reproduces the energy and magnetic characteristics of cobalt complexes with redox-active ligands.^{47,48} Stationary points were located on the potential energy surface (PES) by the

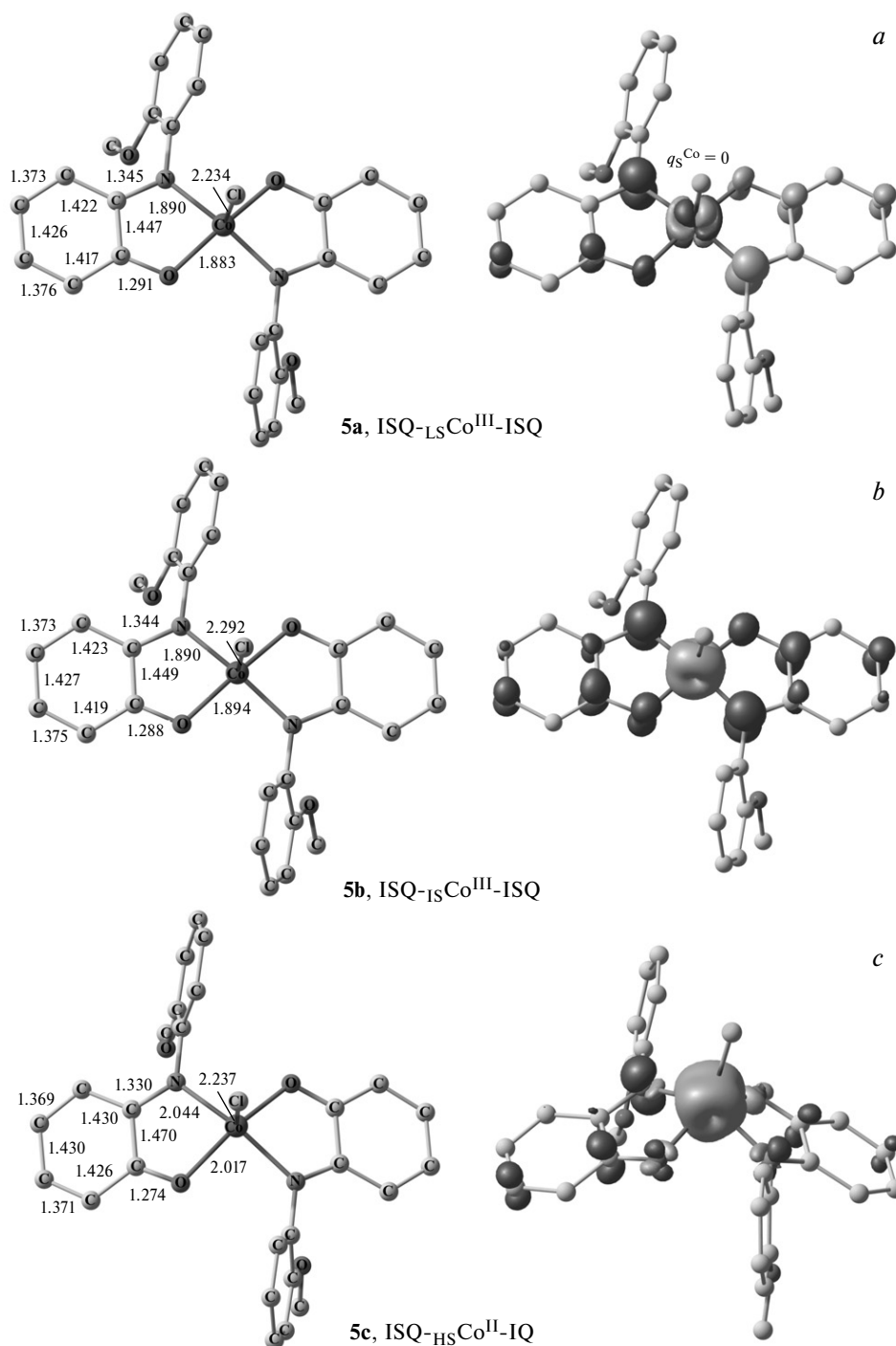


Fig. 7. Geometry of isomers **5a** (a), **5b** (b), and **5c** (c) of the model complex calculated by the DFT method at the UB3LYP*/6-311++G(d,p) level of theory.

full geometry optimization of molecular structures, with checking the stability of DFT wave functions. Exchange interactions between unpaired electrons of paramagnetic centers were evaluated by the broken symmetry (BS) approach.⁴⁹ Exchange interaction parameters (J/cm^{-1}) were calculated using the Yamaguchi formula.⁵⁰ The molecular structures shown in Fig. 7 were visualized using the ChemCraft program.⁵¹

X-ray diffraction studies of compounds 4–7 and 9 were performed on Agilent Xcalibur E (for **4**), Bruker Smart Apex (for **5** and **6**), and Bruker D8 Quest (for **7** and **9**) diffractometers (ω -scanning technique, Mo- $K\alpha$ radiation, $\lambda = 0.71073 \text{ \AA}$, $T = 100 \text{ K}$). The intensity data were measured and integrated, absorption corrections were applied, and the structures were refined using the CrysAlis Pro,⁵² Smart,⁵³ APEX2,⁵⁴ SADABS,⁵⁵

and SHELX program packages.⁵⁶ The structures were solved by direct methods and refined by the full-matrix least squares based on F^2_{hkl} with anisotropic displacement parameters for non-hydrogen atoms. Hydrogen atoms of complexes **4**–**7** and **9** were positioned geometrically and refined isotropically with fixed thermal parameters $U(H)_{\text{iso}} = 1.2U(C)_{\text{eq}}$ ($U(H)_{\text{iso}} = 1.5U(C)_{\text{eq}}$ for methyl groups). The crystallographic data and the X-ray diffraction data collection and refinement statistics are given in Tables 6 and 7. The structures were deposited with the Cambridge Crystallographic Data Centre (CCDC 1486943 (**4**), 1589006 (**5**), 1589008 (**6**), 1589007 (**7**), 1589009 (**9**)) and are available at ccdc.cam.ac.uk/structures.

Chlorobis[4,6-di-*tert*-butyl-*N*-(diphenyl)-*o*-iminobenzosemiquinonato]cobalt(III) (4**).** A solution of $\text{CoCl}_2 \cdot 6\text{H}_2\text{O}$ (0.06 g, 0.27 mmol) in methanol (10 mL) was added to a solution of 4,6-di-*tert*-butyl-*N*-(diphenyl)-*o*-aminophenol (**1**) (0.2 g, 0.54 mmol) in the same solvent (15 mL) placed in an evacuated tube. The reaction mixture was stirred for 10–15 min in the presence of NEt_3 (0.15 mL) without contact with oxygen, resulting in the formation of a pale flocculent precipitate in the bright blue solution. The forcing of atmospheric oxygen into the tube for 10–15 min led to a change in the color of the reaction mixture to intense dark-blue. The slow evaporation of the solvent enabled the formation of a polycrystalline phase composed of two types of crystals (dark-blue needle-like and violet hexagonal). The latter crystals proved to be suitable for X-ray diffraction and had the composition corresponding to compound **4**. Fractional crystallization did not produce analytically pure compound **4** without an impurity of complex **7**. This impurity was evident from the presence of a characteristic

signal in the ESR spectrum identical to that described in the literature.²⁴

Chlorobis[4,6-di-*tert*-butyl-*N*-(2-methoxyphenyl)-*o*-iminobenzosemiquinonato]cobalt(III) (5**).** A solution of 4,6-di-*tert*-butyl-*N*-(2-methoxyphenyl)-*o*-aminophenol (**2**) (0.2 g, 0.61 mmol) was added to a solution of $\text{CoCl}_2 \cdot 6\text{H}_2\text{O}$ (0.07 g, 0.31 mmol) in acetonitrile (15 mL) in an evacuated tube. Then NEt_3 (0.15 mL) was added to the reaction mixture with vigorous stirring without contact with oxygen for 5 min, resulting in the formation of a pale-blue flocculent precipitate in the blue-green solution. The passing of atmospheric oxygen into the tube followed by stirring of the reaction mixture was accompanied by dissolution of the resulting precipitate and a change in the color of the solution to dark-blue. The slow evaporation of the solvent enabled the formation of dark-blue single crystals suitable for X-ray diffraction. The product yield was 0.14 g (61%). Found (%): C, 67.57; H, 7.27. $\text{C}_{42}\text{H}_{54}\text{ClCoN}_2\text{O}_4$. Calculated (%): C, 67.69; H, 7.30. $^1\text{H NMR}$ (200 MHz, CDCl_3 , 20 °C), δ : 1.08 (s, 18 H, Bu^t); 1.16 (s, 18 H, Bu^t); 3.62 (s, 6 H, CH_3); 6.84 (m, 1 H, $\text{C}=\text{CH}$); 6.88 (m, 1 H, $\text{C}=\text{CH}$); 7.09 (m, 2 H, $\text{C}=\text{CH}$); 7.45 (m, 2 H, $\text{C}=\text{CH}$); 7.55 (m, 2 H, $\text{C}=\text{CH}$); 8.54 (m, 4 H, $\text{C}=\text{CH}$). IR, ν/cm^{-1} : 466 w, 482 w, 507 m, 530 m, 553 w, 568 w, 610 m, 619 w, 627 w, 647 m, 665 m, 747 s, 789 m, 833 w, 855 s, 890 m, 913 m, 936 m, 999 s, 1021 s, 1033 m, 1047 s, 1100 m, 1113 s, 1142 w, 1161 m, 1174 s, 1206 s, 1247 s, 1258 s, 1283 w, 1310 s, 1337 m, 1363 s, 1395 m, 1411 w, 1435 m, 1478 w, 1492 s, 1523 m, 1591 m, 1775 w, 3061 w, 3074 w.

Chlorobis[4,6-di-*tert*-butyl-*N*-(2-methylcarboxylatophenyl)-*o*-iminobenzosemiquinonato]cobalt(III) (6**).** Triethylamine (0.15 mL) was added to a solution of methyl 2-(3,5-di-*tert*-butyl-2-hydroxy-

Table 6. Crystallographic data and the X-ray data collection and structure refinement statistics for compounds **4**–**6**

Compound	4 · CH_3CN	5	6 · $2.5\text{CH}_3\text{CN}$
Molecular formula	$\text{C}_{54}\text{H}_{61}\text{ClCoN}_3\text{O}_2$	$\text{C}_{42}\text{H}_{54}\text{ClCoN}_2\text{O}_4$	$\text{C}_{49}\text{H}_{61.50}\text{ClCoN}_{4.50}\text{O}_6$
Molecular weight	878.43	745.25	903.90
Crystal system	Triclinic	Tetragonal	Triclinic
Space group	$P\bar{1}$	$P4_1$	$P\bar{1}$
$a/\text{Å}$	12.5150(3)	15.0634(9)	12.2404(8)
$b/\text{Å}$	14.0269(4)	15.0634(9)	14.6340(9)
$c/\text{Å}$	14.8994(4)	17.1132(10)	14.9869(9)
α/deg	79.329(2)	90	87.0590(10)
β/deg	78.962(2)	90	80.0320(10)
γ/deg	69.409(3)	90	65.3630(10)
$V/\text{Å}^3$	2383.31(12)	3883.1(5)	2402.7(3)
Z	2	4	2
Crystal size/mm	0.62½0.33½0.10	0.08½0.08½0.08	0.45½0.23½0.11
$d_{\text{calc}}/\text{mg m}^{-3}$	1.224	1.275	1.249
μ/mm^{-1}	0.459	0.554	0.464
Number of reflections			
measured	48445	41317	12585
unique	14529	10018	8233
(R_{int})	0.0994	0.0724	0.0192
Number of refined parameters	623	465	572
R_1/wR_2 ($I > 2\sigma(I)$)	0.0718/0.1062	0.0520/0.1017	0.0486/0.1182
R_1/wR_2 (based on all data)	0.1261/0.1220	0.0809/0.1134	0.0677/0.1300
$S(F^2)$	1.029	1.012	1.021
Residual electron density	0.83/–0.69	0.54/–0.22	0.77/–0.39
($\rho_{\text{max}}, \rho_{\text{min}}$)/ e Å^{-3}			

Table 7. Crystallographic data and the X-ray data collection and structure refinement statistics for compounds **7** and **9**

Compound	7	9
Molecular formula	C ₅₂ H ₅₈ CoN ₂ O ₂	C ₄₇ H ₆₁ CoN ₂ O ₆
Molecular weight	801.93	808.90
Crystal system	Triclinic	Monoclinic
Space group	<i>P</i> $\bar{1}$	<i>C</i> 2/ <i>c</i>
<i>a</i> /Å	12.1911(9)	30.373(4)
<i>b</i> /Å	13.7898(11)	9.6687(12)
<i>c</i> /Å	15.1838(12)	18.273(2)
α /deg	106.064(2)	90
β /deg	99.261(2)	125.980(2)
γ /deg	112.0500(10)	90
<i>V</i> /Å ³	2170.7(3)	4342.3(9)
<i>Z</i>	2	4
Crystal size/mm	0.23½0.11½0.08	0.43½0.15½0.08
<i>d</i> _{calc} /mg m ⁻³	1.227	1.237
μ /mm ⁻¹	0.438	0.444
Number of reflections		
measured	30787	23247
unique	12897	5499
(<i>R</i> _{int})	0.0328	0.0371
Number of refined parameters	526	275
<i>R</i> ₁ / <i>wR</i> ₂ (<i>I</i> > 2 σ (<i>I</i>))	0.0445/0.1133	0.0451/0.1161
<i>R</i> ₁ / <i>wR</i> ₂ (based on all data)	0.0578/0.1202	0.0608/0.1263
<i>S</i> (<i>F</i> ²)	1.036	1.036
Residual electron density	0.76/−0.28	0.61/−0.29
(ρ _{max} / ρ _{min})/e Å ⁻³		

phenylamino)benzoate (**3**) (0.2 g, 0.56 mmol) and CoCl₂·6H₂O (0.07 g, 0.28 mmol) in acetonitrile (15 and 10 mL, respectively) in an evacuated tube, which was accompanied by a change in the color of the reaction mixture to dark-blue and the formation of a white flocculent precipitate. The latter was dissolved by vigorous stirring (5–10 min) of the resulting solution after passing of atmospheric oxygen into the tube. Dark crystals of complex **6**·2.5CH₃CN suitable for X-ray diffraction were grown from the resulting dark-blue mixture upon cooling. The product yield was 0.17 g (67%). Found (%): C, 65.28; H, 6.96. C₄₉H_{61.50}ClCoN_{4.50}O₆. Calculated (%): C, 65.10; H, 6.87. IR, ν /cm⁻¹: 465 w, 502 w, 512 m, 541 m, 553 w, 613 w, 622 w, 650 m, 659 w, 669 w, 702 m, 747 s, 770 m, 784 m, 794 m, 815 w, 835 w, 858 m, 875 w, 891 w, 902 m, 915 m, 933 w, 966 m, 999 s, 1032 s, 1042 m, 1086 s, 1103 s, 1134 m, 1163 w, 1182 s, 1205 m, 1233 w, 1259 s, 1294 s, 1310 s, 1339 w, 1365 s, 1396 m, 1412 w, 1434 m, 1480 s, 1524 m, 1573 w, 1596 m, 1723 s, 1732 s, 1776 w, 3070 w.

[4,6-Di-*tert*-butyl-*N*-(diphenyl)-*o*-iminobenzosemiquinonato-4,6-di-*tert*-butyl-*N*-(diphenyl)-*o*-amidophenoxido]cobalt(III) (7**).** A solution of (acac)₂Co·2H₂O (0.08 g, 0.27 mmol) in methanol (10 mL) was added to a solution of 4,6-di-*tert*-butyl-*N*-(diphenyl)-*o*-aminophenol (**1**) (0.2 g, 0.54 mmol) in the same solvent (15 mL) in an evacuated tube. The resulting reaction mixture immediately turned dark-blue after the mixing of the starting reagents. After stirring for 10 min without heating under aerobic conditions, the resulting solution turned intense dark-blue followed by the gradual formation of a dark blue-violet needle-like finely crystalline product. The precipitate

was filtered on a Schott glass filter no. 4 and washed with methanol (10–15 mL). Dark-blue single crystals of the composition of compound **7** were obtained by the recrystallization of the polycrystalline product from toluene under reduced pressure during the slow cooling of the hot solution (\approx 60–70 °C). The product yield (from methanol) was 0.13 g (60%). The spectroscopic characteristics of complex **4** isolated from the reaction mixture are completely identical to those described in the literature.²⁴

[4,6-Di-*tert*-butyl-*N*-(2-methoxyphenyl)-*o*-iminobenzosemiquinonato-4,6-di-*tert*-butyl-*N*-(2-methoxyphenyl)-*o*-amidophenoxido]cobalt(III) (8**) and acetylacetonato-bis[4,6-di-*tert*-butyl-*N*-(2-methoxyphenyl)-*o*-iminobenzosemiquinonato]cobalt(III) (**9**).** A solution of (acac)₂Co·2H₂O (0.09 g, 0.31 mmol) in methanol (10 mL) was added to a solution of 4,6-di-*tert*-butyl-*N*-(2-methoxyphenyl)-*o*-aminophenol (**2**) (0.2 g, 0.61 mmol) in the same solvent (15 mL) in an evacuated tube. After the mixing of the resulting solutions, the reaction mixture turned pale-brown, and the color of the solution immediately changed to intense dark-blue on stirring in the presence of atmospheric oxygen. After 15–20 min, the dark crystalline precipitate began to form. Several single crystals of the composition C₄₇H₆₁CoN₂O₆ (which corresponds to minor compound **9**) proved to be suitable for X-ray diffraction. The anisotropic ESR spectrum of the glassy solution of the crystalline phase in dichloromethane shows a signal, which is similar to that described for compound **7**²⁴ and corresponds to compound **8**. Fractional crystallization did not produce analytically pure compounds **8** and **9**.

This work was financially supported by the Russian Foundation for Basic Research (Project No. 18-33-00539_mol_a). The X-ray diffraction studies were performed within the framework of the State assignment (task No. 44.2, registration number AAAA-A16-116122110053-1) using equipment of the Analytical Center of the G. A. Razuvaev Institute of Organometallic Chemistry of the Russian Academy of Sciences.

References

1. G. A. Abakumov, A. V. Piskunov, V. K. Cherkasov, I. L. Fedushkin, V. P. Ananikov, D. B. Eremin, E. G. Gordeev, I. P. Beletskaya, A. D. Averin, M. N. Bochkarev, A. A. Trifonov, U. M. Dzhemilev, V. A. Dyakonov, M. P. Egorov, A. N. Verezhchagin, M. A. Syroeshkin, V. V. Jouikov, A. M. Muzafarov, A. A. Anisimov, A. V. Arzumanyan, Yu. N. Kononevich, M. N. Temnikov, O. G. Synyashin, Yu. H. Budnikova, A. R. Burirov, A. A. Karasik, V. F. Mironov, P. A. Storozhenko, G. I. Shcherbakova, B. A. Trofimov, S. V. Amosova, N. K. Gusarova, V. A. Potapov, V. B. Shur, V. V. Burlakov, V. S. Bogdanov, M. V. Andreev, *Russ. Chem. Rev.*, 2018, **87**, 393.
2. D. L. J. Broere, R. Plessius, J. I. van der Vlugt, *Chem. Soc. Rev.*, 2015, **44**, 6886.
3. W. I. Dzik, J. I. van der Vlugt, J. N. H. Reek, B. de Bruin, *Angew. Chem., Int. Ed.*, 2011, **50**, 3356.
4. O. R. Luca, R. H. Crabtree, *Chem. Soc. Rev.*, 2013, **42**, 1440.
5. V. Lyaskovskyy, B. de Bruin, *ACS Catal.*, 2012, **2**, 270.
6. I. L. Fedushkin, A. S. Nikipelov, A. G. Morozov, A. A. Skatova, A. V. Cherkasov, G. A. Abakumov, *Chem. Eur. J.*, 2012, **18**, 255.
7. A. V. Piskunov, I. N. Meshcheryakova, G. K. Fukin, A. S. Shavyrin, V. K. Cherkasov, G. A. Abakumov, *Dalton Trans.*, 2013, **42**, 10533.
8. A. V. Piskunov, I. V. Ershova, G. K. Fukin, A. S. Shavyrin, *Inorg. Chem. Commun.*, 2013, **38**, 127.
9. A. V. Piskunov, M. G. Chegerev, G. K. Fukin, *J. Organomet. Chem.*, 2016, **803**, 51.
10. I. L. Fedushkin, V. A. Dodonov, A. A. Skatova, V. G. Sokolov, A. V. Piskunov, *Chem. Eur. J.*, 2018, **24**, 1877.
11. A. I. Poddel'sky, V. K. Cherkasov, G. A. Abakumov, *Coord. Chem. Rev.*, 2009, **253**, 291.
12. M. G. Chegerev, A. V. Piskunov, *Russ. J. Coord. Chem.*, 2018, **44**, 258.
13. M. G. Chegerev, A. V. Piskunov, A. A. Starikova, S. P. Kubrin, G. K. Fukin, V. K. Cherkasov, G. A. Abakumov, *Eur. J. Inorg. Chem.*, 2018, 1087.
14. K. V. Tsys, M. G. Chegerev, G. K. Fukin, A. V. Piskunov, *Mendeleev Commun.*, 2018, **28**, 527.
15. M. G. Chegerev, A. V. Piskunov, K. V. Tsys, A. G. Starikov, K. Jurkschat, E. V. Baranov, A. I. Stash, G. K. Fukin, *Eur. J. Inorg. Chem.*, 2019, 875.
16. A. L. Smith, K. I. Hardcastle, J. D. Soper, *J. Am. Chem. Soc.*, 2010, **132**, 14358.
17. C. N. Verani, S. Gallert, E. Bill, T. Weyhermüller, K. Wieghardt, P. Chaudhuri, *Chem. Commun.*, 1999, 1747.
18. A. I. Poddel'sky, V. K. Cherkasov, G. K. Fukin, M. P. Bubnov, L. G. Abakumova, G. A. Abakumov, *Inorg. Chim. Acta*, 2004, **357**, 3632.
19. A. L. Smith, L. A. Clapp, K. I. Hardcastle, J. D. Soper, *Polyhedron*, 2010, **29**, 164.
20. A. V. Piskunov, K. I. Pashanova, A. S. Bogomyakov, I. V. Smolyaninov, A. G. Starikov, G. K. Fukin, *Dalton Trans.*, 2018, **47**, 15049.
21. S. Mukherjee, E. Rentschler, T. Weyhermüller, K. Wieghardt, P. Chaudhuri, *Chem. Commun.*, 2003, 1828.
22. E. Bill, E. Bothe, P. Chaudhuri, K. Chlopek, D. Herebian, S. Kokatam, K. Ray, T. Weyhermüller, F. Neese, K. Wieghardt, *Chem. Eur. J.*, 2005, **11**, 204.
23. P. Chaudhuri, R. Wagner, U. Pieper, B. Biswas, T. Weyhermüller, *Dalton Trans.*, 2008, 1286.
24. G. C. Paul, S. Ghorai, C. Mukherjee, *Chem. Commun.*, 2017, **53**, 8022.
25. M. K. Mondal, A. Tiwari, C. Mukherjee, *Chem. Commun.*, 2016, **52**, 11995.
26. R. Rakshit, S. Ghorai, A. Sarmah, A. Tiwari, R. K. Roy, C. Mukherjee, *Dalton Trans.*, 2015, **44**, 3724.
27. P. Sarkar, A. Tiwari, A. Sarmah, S. Bhandary, R. K. Roy, C. Mukherjee, *Chem. Commun.*, 2016, **52**, 10613.
28. F. D. Lesh, R. L. Lord, M. J. Heeg, H. B. Schlegel, C. N. Verani, *Eur. J. Inorg. Chem.*, 2012, 463.
29. S. Maity, S. Kundu, S. Bera, T. Weyhermüller, P. Ghosh, *Eur. J. Inorg. Chem.*, 2016, 3680.
30. L. M. Kustov, A. L. Kustov, V. B. Kazansky, *Mendeleev Commun.*, 2018, **28**, 354.
31. L. Yang, D. R. Powell, R. P. Houser, *Dalton Trans.*, 2007, 955.
32. A. V. Piskunov, K. I. Pashanova, A. S. Bogomyakov, I. V. Smolyaninov, N. T. Berberova, G. K. Fukin, *Polyhedron*, 2016, **119**, 286.
33. S. N. Brown, *Inorg. Chem.*, 2012, **51**, 1251.
34. A. W. Addison, T. N. Rao, J. Reedijk, J. van Rijn, G. C. Verschoor, *Dalton Trans.*, 1984, 1349.
35. A. V. Piskunov, I. V. Ershova, M. V. Gulenova, K. I. Pashanova, A. S. Bogomyakov, I. V. Smolyaninov, G. K. Fukin, V. K. Cherkasov, *Russ. Chem. Bull.*, 2015, **64**, 642.
36. S. S. Batsanov, *Russ. J. Inorg. Chem.*, 1991, **36**, 1694.
37. D. Herebian, P. Ghosh, H. Chun, E. Bothe, T. Weyhermüller, K. Wieghardt, *Eur. J. Inorg. Chem.*, 2002, 1957.
38. G. A. Abakumov, V. K. Cherkasov, M. P. Bubnov, L. G. Abakumova, V. N. Ikorskii, G. V. Romanenko, A. I. Poddel'skii, *Russ. Chem. Bull.*, 2006, **55**, 44.
39. A. I. Poddel'sky, M. P. Bubnov, G. K. Fukin, V. K. Cherkasov, G. A. Abakumov, *Z. Anorg. Allg. Chem.*, 2008, **634**, 1205.
40. M. Calligaris, G. Manzini, G. Nardin, L. Randaccio, *J. Chem. Soc., Dalton Trans.*, 1972, 543.
41. T. Bally, *Nat. Chem.*, 2010, **2**, 165.
42. V. Bachler, G. Olbrich, F. Neese, K. Wieghardt, *Inorg. Chem.*, 2002, **41**, 4179.
43. S. Ghorai, C. Mukherjee, *Chem. Commun.*, 2012, **48**, 10180.
44. A. J. Gordon, R. A. Ford, *The Chemist's Companion*, Wiley Intersci. Publ., New York, 1972, 537 p.
45. M. J. Frisch, G. W. Trucks, H. B. Schlegel, G. E. Scuseria, M. A. Robb, J. R. Cheeseman, G. Scalmani, V. Barone, B. Mennucci, G. A. Petersson, H. Nakatsuji, M. Caricato, X. Li, H. P. Hratchian, A. F. Izmaylov, J. Bloino, G. Zheng, J. L. Sonnenberg, M. Hada, M. Ehara, K. Toyota, R. Fukuda, J. Hasegawa, M. Ishida, T. Nakajima, Y. Honda, O. Kitao, H. Nakai, T. Vreven, J. A. Montgomery, Jr., J. E. Peralta, F. Ogliaro, M. Bearpark, J. J. Heyd, E. Brothers, K. N. Kudin,

- V. N. Staroverov, T. Keith, R. Kobayashi, J. Normand, K. Raghavachari, A. Rendell, J. C. Burant, S. S. Iyengar, J. Tomasi, M. Cossi, N. Rega, J. M. Millam, M. Klene, J. E. Knox, J. B. Cross, V. Bakken, C. Adamo, J. Jaramillo, R. Gomperts, R. E. Stratmann, O. Yazyev, A. J. Austin, R. Cammi, C. Pomelli, J. W. Ochterski, R. L. Martin, K. Morokuma, V. G. Zakrzewski, G. A. Voth, P. Salvador, J. J. Dannenberg, S. Dapprich, A. D. Daniels, O. Farkas, J. B. Foresman, J. V. Ortiz, J. Cioslowski, D. J. Fox, *Gaussian 09 (Revision E.01)*, Gaussian, Inc., Wallingford CT, 2013.
46. M. Reiher, O. Salomon, B. A. Hess, *Theor. Chem. Acc.*, 2001, **107**, 48.
47. M. Yu. Antipin, E. P. Ivakhnenko, Yu. V. Koshchlenko, P. A. Knyazev, M. S. Korobov, A. V. Chernyshev, K. A. Lyssenko, A. G. Starikov, V. I. Minkin, *Russ. Chem. Bull.*, 2013, **62**, 1744.
48. V. I. Minkin, A. G. Starikov, A. A. Starikova, *Pure Appl. Chem.*, 2018, **90**, 811.
49. L. Noodleman, *J. Chem. Phys.*, 1981, **74**, 5737.
50. Y. Kitagawa, T. Saito, Y. Nakanishi, Y. Kataoka, T. Matsui, T. Kawakami, M. Okumura, K. Yamaguchi, *J. Phys. Chem. A.*, 2009, **113**, 15041.
51. Chemcraft, Version 1.7, 2013: <http://www.chemcraftprog.com>.
52. Agilent (2014). *CrysAlis Pro*. Agilent Technologies Ltd, Yarnton, Oxfordshire, England.
53. Bruker (2012). *Smart*. Bruker AXS Inc., Madison, Wisconsin, USA.
54. Bruker (2014). *APEX2*. Bruker AXS Inc., Madison, Wisconsin, USA.
55. L. Krause, R. Herbst-Irmer, G. M. Sheldrick, D. Stalke, *J. Appl. Cryst.*, 2015, **48**, 3.
56. G. M. Sheldrick, *Acta Cryst.*, 2015, **C71**, 3.

*Received November 1, 2018;
in revised form February 26, 2019;
accepted February 27, 2019*